

CHAPTER IV

ESTIMATION OF THE OPEN-LOOP TRANSFER
FUNCTION OF THE TURBO-ALTERNATOR

This chapter deals with the estimation of the open-loop (i.e. the feedback loop employing governor is disconnected) transfer function of a turbo-alternator of an inter-connected power system from the normal operating input-output data. The state variable formulation of the open-loop plant is first obtained and using the basic theory developed in Chapter III, a suitable algorithm for numerical computation to seek the minima of the performance index is developed using input-output of a simulated system. The same technique is then employed to estimate the parameters (of transfer function) of the plant using the actual operating data. The effect of dynamic noise, not considered in the basic formulation of the estimation problem in Chapter III, is overcome by digital filtering.

4.1 Description of the Plant

The basic equations obtained for the dynamic performance of a synchronous alternator are nonlinear⁹⁸. However, if these equations are linearized by considering small perturbations about the normal operating level, it is possible to represent the dynamic behaviour⁹⁰ of the turbo-alternator by the block diagram depicted in Fig. 4.1. The input and output of the plant are respectively the power demand fluctuations Δp (per unit value) and the corresponding frequency variations $\Delta \omega$ (cycles per second). The frequency of a.c. output from the turbo-alternator has to be maintained within permissible limits about the declared frequency. The variations in frequency are therefore normally counteracted by a feedback loop employing governor which regulates the flow

of steam to the turbine to even out the power load fluctuations. It is required to estimate the parameters of turbo-alternator transfer functions when

- (a) the feedback loop employing governor is kept open - which is termed "open-loop" plant, and
- (b) the feedback loop is closed as normal - which is termed "closed-loop" plant.

The input-output data was therefore made available for both the cases.

The open-loop plant is assumed to be of first order, with the open-loop gain and one time constant to be estimated from the given input-output record for the open-loop plant. In fact, this is the subject matter of this chapter.

While considering the estimation of closed-loop plant from the corresponding input-output data, the feedback loop employing governor is assumed to be

- (i) of first order which involves the estimation of feedback loop gain and one time constant, and alternatively,
- (ii) of second order which requires the estimation of feedback loop gain and two time constants.

The representation of the feed-back loop by two time-constants is more typical. The estimation of closed-loop transfer function involves constants of forward loop and feedback loop. Thus the closed-loop systems corresponding to cases (i) and (ii) above are of second and third order respectively. These are dealt with in Chapter V and VI respectively.

In view of the above discussion, the transfer function of the open-loop plant (shown in Fig. 4.1) is given by

$$\frac{\Delta \Omega(s)}{\Delta P(s)} = \frac{1}{D(1 + \gamma_m s)} \quad (4.1)$$

where 's' is the Laplace Transform variable and $\Delta \Omega(s)$ and $\Delta P(s)$ are the Laplace Transforms of $\Delta \omega(t)$ and $\Delta p(t)$ respectively. The random disturbances with $\Delta \omega(t)$ and $\Delta p(t)$ are ignored for the validity of equality sign in equation (4.1). The parameter D is the composite rotor damping coefficient in per unit/cycles per second and γ_m is the time-constant in seconds of the alternator. Alternatively, $1/D$ represents the open-loop gain. The coefficients K and γ_g are the gain and time-constant for the feedback loop. The four coefficients, viz. D, γ_m , K and γ_g were estimated by Stanton⁹⁰ using power spectra analysis and their estimated values are

$$D = 0.055 \text{ p.u./ c/s} \quad (4.2)$$

$$\gamma_m = 2.5 \text{ secs.} \quad (4.3)$$

$$K = 0.35 \text{ p.u./ c/s} \quad (4.4)$$

$$\gamma_g = 2.5 \text{ secs.} \quad (4.5)$$

Since the quantities Δp and $\Delta \omega$ were found to be very small, they were amplified for convenience by a factor of 1200 and 10^4 respectively before they were measured. The amplified or measured values are given by

$$\Delta \omega' = 1200 \Delta \omega \quad (4.6)$$

$$\Delta p' = 10^4 \Delta p \quad (4.7)$$

The open-loop transfer function in terms of the amplified values

is given by

$$\frac{\Delta \Omega'(s)}{\Delta P'(s)} = \frac{1200 \Delta \Omega(s)}{10^4 \Delta P(s)} \quad (4.8)$$

Using equation (4.1), this becomes

$$\frac{\Delta \Omega'(s)}{\Delta P'(s)} = \frac{1}{D'(1 + \tau_m s)} \quad (4.9)$$

where

$$D' = \frac{10^4}{1200} D \quad (4.10)$$

Thus, if one uses the amplified data, the open-loop gain is obtained as $1/D'$. The value of D' according to Stanton's estimate is readily obtained by using equations (4.2) and (4.10) as

$$D' = 0.458 \text{ p.u./ c/s} \quad (4.11)$$

The problem to be considered in this chapter is to estimate the values of D' and τ_m in equation (4.9) using the same input-output data (amplified) as used by Stanton employing the technique developed in Chapter III. The technique requires the plant dynamics to be represented in terms of state variables as will be discussed in the following section.

4.2 State Variable Formulation

As an intermediate step towards obtaining the state variable formulation⁹⁹, let the open-loop plant transfer function of equation (4.9) be transformed into a differential equation given by

$$\frac{d}{dt} (\Delta \omega') = -\frac{1}{\tau_m} \Delta \omega' + \frac{1}{D \tau_m} \Delta p' \quad (4.12)$$

Using the usual notations, let

$$x_1 = \Delta \omega' \quad (4.13)$$

and

$$u = \Delta p' \quad (4.14)$$

where $x_1 = x_1(t)$ is the true state (ignoring disturbances in the output $\Delta \omega'$ for the time-being) of the system. Substituting these in equation (4.12), one obtains

$$\dot{x}_1 = -\frac{1}{\gamma_m} x_1 + \frac{1}{D' \gamma_m} u \quad (4.15)$$

In order to apply directly the method developed in Chapter III for estimation of constant parameters γ_m and D' , let

$$x_2 = 1/\gamma_m \quad (4.16)$$

and

$$x_3 = 1/D' \quad (4.17)$$

Thus the differential equations representing the dynamics of the plant become

$$\dot{x}_1 = -x_1 x_2 + x_2 x_3 u \quad (4.18)$$

$$\dot{x}_2 = 0 \quad (4.19)$$

$$\dot{x}_3 = 0 \quad (4.20)$$

Equations (4.19) and (4.20) imply that x_2 and x_3 are constants.

These three equations can be brought into the vector form of equation (3.1) by writing

$$x(t) = \text{col} [x_1(t), x_2(t), x_3(t)] \quad (4.21)$$

The true state x_1 ignores the random disturbances and represents the theoretical output $\Delta \omega'$. However, the observed values of x_1 or $\Delta \omega'$ are corrupted with random disturbances

including measurement noise as well as dynamic noise of the system. Thus the discretely measured output $y(i)$ is given by

$$y(i) = x_1(i) + n(i) \quad i = 0, 1, \dots, N \quad (4.22)$$

where $n(i)$ represents the additive noise (at the output) and includes measurement noise and other random disturbances but not the correlated dynamic noise. Since only one state is observable, $y(i)$ is a scalar quantity. Comparison of equation (4.22) with equation (3.3) gives

$$H = (1, 0, 0) \quad (4.23)$$

which is a row vector, and

$$x(i) = \text{col} [x_1(i), x_2(i), x_3(i)] \quad (4.24)$$

represents the state vector of the plant at an instant i .

The problem is to estimate the initial states $x_1(0)$, $x_2(0)$ and $x_3(0)$ from the observations of the input $u(i)$ (power demand fluctuations $\Delta p'$) and the output $y(i)$ (frequency fluctuations $\Delta \omega'$) for $i = 0$ to N .

4.3 Estimation Scheme

The best estimate of $x_1(0)$, $x_2(0)$, $x_3(0)$ is obtained by minimizing the performance index I given by

$$I = \sum_{i=0}^N \Omega [y(i) - \bar{x}_1(i)]^2 \quad (4.25)$$

which is obtained by substituting for H from equation (4.23) in equation (3.11). Here, $\bar{x}_1(i)$ is the nominal trajectory

(i.e. computed output $\bar{y}(i)$) of the dynamic model of the system

simulated on the digital computer) and is obtained by solving the differential equations of the dynamic model given by

$$\dot{\bar{x}}_1 = -\bar{x}_1 \bar{x}_2 + \bar{x}_2 \bar{x}_3 u \quad (4.26)$$

$$\dot{\bar{x}}_2 = 0 \quad (4.27)$$

$$\dot{\bar{x}}_3 = 0 \quad (4.28)$$

for some initial conditions $\bar{x}_1(0)$, $\bar{x}_2(0)$ and $\bar{x}_3(0)$ and the same input as that of the system whose parameters are to be estimated. It should be noted that Q is scalar in the equation (4.25). The above three equations are represented by the general vector differential equation (3.41). The minimization of I in equation (4.25) must satisfy the Euler-Lagrange difference equations and the natural boundary conditions given by equations (3.17) to (3.20). Splitting these into scalar difference equations (noting that the state vector under consideration is 3-dimensional), one obtains

$$\bar{x}_1(i+1) = f_1 [\bar{x}_1(i), \bar{x}_2(i), \bar{x}_3(i), i] \quad (4.29)$$

$$\bar{x}_2(i+1) = f_2 [\bar{x}_1(i), \bar{x}_2(i), \bar{x}_3(i), i] \quad (4.30)$$

$$= \bar{x}_2(i) \quad (4.31)$$

$$\bar{x}_3(i+1) = f_3 [\bar{x}_1(i), \bar{x}_2(i), \bar{x}_3(i), i] \quad (4.32)$$

$$= \bar{x}_3(i) \quad (4.33)$$

and

$$\begin{aligned} \lambda_1(i-1) = & f_{\bar{x}(i)}^{11} \lambda_1(i) + f_{\bar{x}(i)}^{21} \lambda_2(i) + f_{\bar{x}(i)}^{31} \lambda_3(i) \\ & + 2Q [y(i) - \bar{x}_1(i)] \end{aligned} \quad (4.34)$$

$$\lambda_2(i-1) = f_{\bar{x}(i)}^{12} \lambda_1(i) + f_{\bar{x}(i)}^{22} \lambda_2(i) + f_{\bar{x}(i)}^{32} \lambda_3(i) \quad (4.35)$$

$$\lambda_3(i-1) = f_{\bar{x}(i)}^{13} \lambda_1(i) + f_{\bar{x}(i)}^{23} \lambda_2(i) + f_{\bar{x}(i)}^{33} \lambda_3(i) \quad (4.36)$$

with the following boundary conditions

$$\lambda_k(-1) = 0 \quad ; k = 1, 2, 3 \quad (4.37)$$

$$\lambda_k(N) = 0 \quad ; k = 1, 2, 3 \quad (4.38)$$

Equations (4.29), (4.31) and (4.33) are discrete-time version of equations (4.26) to (4.28) and are not available in the closed form when the values $\bar{x}_1(i)$, $\bar{x}_2(i)$ and $\bar{x}_3(i)$ are obtained by numerical integration of equations (4.26) to (4.28). Equations (4.31) and (4.33) imply that $\bar{x}_2(i)$ and $\bar{x}_3(i)$ are constants.

The Jacobian matrix elements $f_{\bar{x}(i)}^{jk}$ required in equations

(4.34) to (4.36) are to be computed by solving equation (3.46).

The matrix $g_{\bar{x}}$ corresponding to equations (4.26), (4.27) and

(4.28) is given by

$$g_{\bar{x}} = \begin{bmatrix} -\bar{x}_2 & -\bar{x}_1 + \bar{x}_3 u & \bar{x}_2 u \\ 0 & 0 & 0 \\ 0 & 0 & 0 \end{bmatrix} \quad (4.39)$$

The state transition matrix $\bar{\Phi}(i+1, i)$ of equation (3.46) is a 3×3 matrix in the present case and its $(j, k)^{th}$ element is written as $\phi^{jk}(i+1, i)$. Substituting for $g_{\bar{x}}$ from equation (4.39) in equation (3.46) and then performing the vector multiplication, one obtains a scalar equation for each element of

$\Phi(i+1, i)$ as follows.

$$\begin{aligned} \dot{\phi}^{11}(i+1, i) &= -\bar{x}_2 \phi^{11}(i+1, i) + (-\bar{x}_1 + \bar{x}_3 u) \phi^{21}(i+1, i) \\ &\quad + \bar{x}_2 u \phi^{31}(i+1, i) ; \phi^{11}(i, i) = 1 \end{aligned} \quad (4.40)$$

$$\begin{aligned} \dot{\phi}^{12}(i+1, i) &= -\bar{x}_2 \phi^{13}(i+1, i) + (-\bar{x}_1 + \bar{x}_3 u) \phi^{22}(i+1, i) \\ &\quad + \bar{x}_2 u \phi^{32}(i+1, i) ; \phi^{12}(i, i) = 0 \end{aligned} \quad (4.41)$$

$$\begin{aligned} \dot{\phi}^{13}(i+1, i) &= -\bar{x}_2 \phi^{13}(i+1, i) + (-\bar{x}_1 + \bar{x}_3 u) \phi^{23}(i+1, i) \\ &\quad + \bar{x}_2 u \phi^{33}(i+1, i) ; \phi^{13}(i, i) = 0 \end{aligned} \quad (4.42)$$

$$\dot{\phi}^{21}(i+1, i) = 0 ; \phi^{21}(i, i) = 0 \quad (4.43)$$

$$\dot{\phi}^{22}(i+1, i) = 0 ; \phi^{22}(i, i) = 1 \quad (4.44)$$

$$\dot{\phi}^{23}(i+1, i) = 0 ; \phi^{23}(i, i) = 0 \quad (4.45)$$

$$\dot{\phi}^{31}(i+1, i) = 0 ; \phi^{31}(i, i) = 0 \quad (4.46)$$

$$\dot{\phi}^{32}(i+1, i) = 0 ; \phi^{32}(i, i) = 0 \quad (4.47)$$

$$\dot{\phi}^{33}(i+1, i) = 0 ; \phi^{33}(i, i) = 1 \quad (4.48)$$

The state transition matrix represents the Jacobian matrix by virtue of equation (3.47). The dynamic equations (4.26) to (4.28) and the equations from (4.40) to (4.48) together can be integrated simultaneously between the successive sampling instants (to obtain the nominal trajectory and the Jacobian matrix respectively) by using AMRK¹⁰⁰ subroutine. The AMRK subroutine has been specially programmed to solve n first order simultaneous differential equations. However, the equations (4.43) to (4.48)

imply that the Jacobian matrix elements $f_{\bar{x}(i)}^{21}$, $f_{\bar{x}(i)}^{22}$, $f_{\bar{x}(i)}^{23}$, $f_{\bar{x}(i)}^{31}$, $f_{\bar{x}(i)}^{32}$, $f_{\bar{x}(i)}^{33}$ are constants and are respectively 0, 1, 0, 0, 0, 1. This is obvious from equations (4.31) and (4.33) which also suggest that equations (4.27) and (4.28) need not be integrated since $\bar{x}_2(i) = \bar{x}_2(0)$ and $\bar{x}_3(i) = \bar{x}_3(0)$ for $i = 1, 2, \dots, (N+1)$. The equations (4.27), (4.28) and (4.43) to (4.48) may therefore be excluded from the AMRK subroutine to save computer time.

The entire computational procedure is outlined as follows:

1. Make an initial guess on the initial conditions

$$\bar{x}_1(0), \bar{x}_2(0) \text{ and } \bar{x}_3(0).$$

2. Integrate (numerically using AMRK) equation (4.26) to obtain $\bar{x}_1(i)$ and equations (4.40) to (4.42) to obtain the Jacobian matrix elements $f_{\bar{x}(i)}^{11}$, $f_{\bar{x}(i)}^{12}$ and $f_{\bar{x}(i)}^{13}$; $i = 0$ to N . The values of $\bar{x}_2(i)$, $\bar{x}_3(i)$ and other elements of Jacobian matrix are known as discussed before.

3. Compute the performance index I using equation (4.25).

The value of Q is taken to be 100.

- 4a. If the current value of I is less than the previous value of I , compute $\lambda_1(-1)$, $\lambda_2(-1)$, $\lambda_3(-1)$ from equations (4.34) to (4.36) starting with $\lambda_1(N) = \lambda_2(N) = \lambda_3(N) = 0$.

Then modify that values of initial conditions by the following rule as per equation (3.48).

$$\text{new } \bar{x}_1(0) = \text{old } \bar{x}_1(0) + \left[\frac{\Delta A}{\sqrt{\sum_{k=1}^3 \lambda_k^2(-1)}} \right] \lambda_1(-1) \quad (4.49)$$

$$\text{new } \bar{x}_2(0) = \text{old } \bar{x}_2(0) + [\quad " \quad] \lambda_2(-1) \quad (4.50)$$

$$\text{new } \bar{x}_3(0) = \text{old } \bar{x}_3(0) + [\quad " \quad] \lambda_3(-1) \quad (4.51)$$

The step-size ΔA is chosen to be 0.1 to start with.

Go back to step (2) above and repeat the sequence.

This procedure is followed until I becomes minimum in which case the initial states $\bar{x}_1(0)$, $\bar{x}_2(0)$ and $\bar{x}_3(0)$ are expected to have converged to their true values.

The above computational procedure will be first shown to work successfully with the input-output data obtained from a computer-simulated system as discussed in the following section.

4.4 Estimation from Input-Output Record of a Computer-Simulated System Similar to Open-loop Plant

While working on an estimation problem under actual operating conditions, one has to make sure that the values of states and parameters estimated are close to their true values. The assurance of correct estimation depends upon the confidence one has gained in the estimation technique used. To ensure feasibility of the technique, it must be first tried out for estimation from input-output data obtained for a computer-simulated system in which case one is in a position to compare estimated values with the known true values. A transfer function of the form

$$G(s) = \frac{1}{0.5(1 + 2.5s)} \quad (4.51)$$

which is somewhat similar to the open-loop plant transfer function (estimated by Stanton) and which gives rise to differential equations (4.18), (4.19) and (4.20) with $x_2(0) = 0.4$ and $x_3(0) = 2.0$, was simulated on the digital computer. The output was obtained with a sampling interval of 0.125 sec., considering sinusoidal input and the initial condition $x_1(0) = 0.2$. The sampling period was chosen to be the same as that for input of the experimental data. This output combined with or without additive noise (generated by using RRN¹⁰¹) and the sinusoidal input were then used to perform several experiments aimed at getting suitable algorithm for best estimate of initial states $x_1(0)$, $x_2(0)$ and $x_3(0)$. The RRN subroutine generates random numbers with a rectangular distribution.

During the early stages of experimentation (without considering noise) it was realized that increasing the number of measurements of input-output speeded up the rate of convergence and also resulted in better estimates of the initial states. It was also concluded that too small a value of the step-size ΔA slowed down the convergence whereas with large values of ΔA , the convergence was faster in the beginning but kept on fluctuating around the minima in the later stages. It was found most expedient to let $\Delta A = 0.1$ in the beginning and then halving it whenever the value of performance index I of the current equation exceeded that of the previous iteration. This gave faster convergence. If the difference between two successive

values of I is very small, inspite of considerable changes in variables $\bar{x}_1(0)$, $\bar{x}_2(0)$ and $\bar{x}_3(0)$ on each iteration, the computer program run stops at such a stage giving an impression of a minima. This situation is known as the plateau problem. This deceptive situation was avoided by taking large steps along the gradient. Large steps helped in jumping over the plateau region. Thus a suitable computational algorithm was developed. As such the step (4) of the computational procedure on page 85 is supplemented by the following instruction.

4b. If the current value of I is greater than its previous value, go back to previous iteration and reduce step-size ΔA to $\Delta A/2$ and modify $\bar{x}_1(0)$, $\bar{x}_2(0)$ and $\bar{x}_3(0)$ using stored previous values of $\lambda_1(-1)$, $\lambda_2(-1)$ and $\lambda_3(-1)$ in equations (4.49), (4.50) and (4.51). And go back to step (2).

4c. If the current value of I is almost equal to the previous value of I , modify $\bar{x}_1(0)$, $\bar{x}_2(0)$ and $\bar{x}_3(0)$ by taking large value of ΔA along the gradient. If this fails to locate I lower than the previous one, stop computation.

Several computer runs were made considering different conditions of noise and these experiments have been catagorized into the following two cases with subcases for each.

CASE I Estimation of initial states $x_1(0)$, $x_2(0)$, $x_3(0)$ from measurements of $x_1(i)$ (a) without additive noise,

(b) with the noise having zero mean, (c) with the noise having nonzero mean.

The true state $x_1(i)$ for $i = 0$ to 94 was computed using equations (4.18), (4.19) and (4.20) for $x_1(0) = 0.2$, $x_2(0) = 0.4$, $x_3(0) = 2.0$ and sinusoidal input $u(i) = 1 \times \sin(0.125 i)$ with a sampling interval of 0.125 seconds. The output $y(i)$ may be of three categories:

- (a) Without Additive Noise : The output $y(i)$ without additive noise was obtained as $y(i) = x_1(i)$, $i = 0$ to 94 (i.e. 95 measurements).
- (b) With the Additive Noise Having Zero Mean : Ninety five random numbers representing noise were generated by using RRN subroutine and stored separately. The values of these numbers were kept within the bounds ± 0.05 . Comparing this magnitude with the unity amplitude of sinusoidal input, the noise level is termed as 5%. This had a nonzero mean. The mean of these 95 numbers was computed and deducted from each of them. The new set of random numbers has zero mean. These numbers were then added to $x_1(i)$'s to obtain the output $y(i)$ with additive noise having zero mean. This noise includes all random disturbances (including measurement noise), appearing additively at the output. It does not represent dynamic noise of the system.
- (c) With the Additive Noise Having Nonzero Mean : The output $y(i)$ having nonzero mean is obtained by adding

to $x_1(i)$ the random numbers generated by RRN.

The input and output of each of the above three cases were used for estimation of $x_1(0)$, $x_2(0)$ and $x_3(0)$ following the computational procedure discussed earlier. Figures 4.2, 4.3 and 4.4 show the convergence of $\bar{x}_1(0)$, $\bar{x}_2(0)$ and $\bar{x}_3(0)$ respectively towards their true values for the three different conditions of output as discussed in (a), (b) and (c) above. The initial guess in each case were $\bar{x}_1(0) = y(0)$, $\bar{x}_2(0) = 0$, $\bar{x}_3(0) = 0$. The estimated values are shown in Table 4.1.

Table 4.1 Estimated Values of Initial States for a Computer-Simulated System Similar to the Open-loop Plant. *CASE I*

	$x_1(0)$	$x_2(0)$	$x_3(0)$
(1) True Values	0.2	0.4	2.0
Estimated Values for			
(2) No Noise	0.214	0.403	1.947
(3) Noise having zero mean	0.216	0.406	1.982
(4) Noise having nonzero mean	0.193	0.466	1.759
Mean of Noise = - 0.058			

These results indicate that better estimates are obtained only when there is either no noise or when the noise has zero mean. When the noise does not have zero mean, the estimated values of $x_2(0)$ and $x_3(0)$ are far off from their true values. This is also evident from the following analytical proof.

The true state $x_1(i)$ is observed in the output as per equation (4.22), i.e.

$$y(i) = x_1(i) + n(i) \quad i = 0, 1, \dots, N \quad (4.52)$$

The best estimate of the initial state $x(0)$ is obtained by fitting the nominal trajectory $\bar{x}_1(i)$ on $y(i)$ in the least squares sense. Thus the performance criterion to be minimized (equation (4.25)) is

$$I = \sum_{i=0}^N Q [y(i) - \bar{x}_1(i)]^2 \quad ; \quad Q > 0 \quad (4.53)$$

Differentiating I w.r.t. $x_1(i)$ and equating the result to zero for minima, this becomes

$$- 2 Q \sum_{i=0}^N [y(i) - \bar{x}_1(i)] = 0 \quad (4.54)$$

Adding and subtracting $\bar{x}_1(i)$ within the brackets and dividing by $2Q(N+1)$ on either side of equation (4.54) and rearranging the terms, this becomes

$$\frac{1}{N+1} \sum_{i=0}^N [x_1(i) - \bar{x}_1(i)] = \frac{1}{N+1} \sum_{i=0}^N [y(i) - \bar{x}_1(i)] \quad (4.55)$$

The mean or expectation of noise $n(i)$, $i = 0, 1, \dots, N$ is given by

$$n_m = \frac{1}{N+1} \sum_{i=0}^N n(i) \quad (4.56)$$

Using this in equation (4.55), one obtains

$$\frac{1}{N+1} \sum_{i=0}^N [x_1(i) - \bar{x}_1(i)] = n_m \quad (4.57)$$

Equation (4.57) indicates that, if the noise has zero mean, the best fit $\bar{x}_1(i)$ on $y(i)$ is almost the same as the true trajectory $x_1(i)$. This is shown in Fig. 4.5. Since $\bar{x}_1(i)$ depends on $\bar{x}_1(0)$, $\bar{x}_2(0)$ and $\bar{x}_3(0)$, the best $\bar{x}_1(i)$ also gives the best estimate of these initial conditions. The equation (4.57)

also evidences that if the noise does not have zero mean, the estimated trajectory (i.e. best $\bar{x}_1(i)$) will be away from the true one by the amount equal to the mean of noise. Thus the estimation is in error. This is depicted in Fig. 4.6.

To overcome the difficulty posed by nonzero mean of noise, several experiments were made and they are discussed in case II.

CASE II Estimation of Initial States $x_1(0)$, $x_2(0)$ and $x_3(0)$ From Measurements of $x_1(i)$ Computed with Noise (Having Nonzero Mean) Considering the Mean of Noise Separately in Three Different Ways.

The general estimation procedure followed for this case was more or less the same as that of case I. The output $y(i)$, $i = 0$ to 94 with the additive noise having nonzero mean for the sinusoidal input was obtained for the same system as described in case I. The nonzero mean of noise which gave wrong estimates is tackled by three different methods.

Method (a)

After having computed the nominal trajectory $\bar{x}_1(i)$ from the initial guesses $\bar{x}_1(0) = y(0)$, $\bar{x}_2(0) = 0$, $\bar{x}_3(0) = 0$, the mean of residual error e_m was computed as

$$e_m = \frac{1}{N+1} \sum_{i=0}^N [y(i) - \bar{x}_1(i)] \quad (4.58)$$

The performance index I to be minimized was then modified to

$$I = \sum_{i=0}^N \Omega [y(i) - \bar{x}_1(i) - e_m]^2 \quad (4.59)$$

Consequently the equation (4.34) had to be changed as follows:

$$\lambda_1(i-1) = \frac{f^{11}}{\bar{x}(i)} \lambda_1(i) + \frac{f^{21}}{\bar{x}(i)} \lambda_2(i) + \frac{f^{31}}{\bar{x}(i)} \lambda_3(i) + 2 \Omega [y(i) - \bar{x}_1(i) + e_m] \quad (4.60)$$

The equations for $\lambda_2(i)$ and $\lambda_3(i)$ remained unchanged. The estimated values for $x_1(0)$, $x_2(0)$ and $x_3(0)$ shown in Figures 4.7, 4.8 and 4.9 are better than corresponding values of Case I. The mean e_m of residual errors finally converges to the mean n_m of noise. The estimated values are given in Table 4.2.

Method (b)

A fourth state variable x_4 was introduced to take care of the mean of noise, i.e.

$$x_4 = n_m \quad (4.61)$$

Thus a fourth equation given by

$$\dot{x}_4 = 0 \quad (4.62)$$

is added to the three differential equations (4.18), (4.19) and (4.20). The state $x_1(i)$ was observed (equation (4.22)) as

$$y(i) = x_1(i) + n(i) \quad i = 0, 1, \dots, N \quad (4.63)$$

The noise $n(i)$ has nonzero mean in this case. It can be written as

$$\begin{aligned} n(i) &= n'(i) + n_m \\ &= n'(i) + x_4(i) \end{aligned} \quad (4.64)$$

where $n'(i)$ is the noise with zero mean. Therefore

$$y(i) = x_1(i) + x_4(i) + n'(i) \quad (4.65)$$

One more differential equation in addition to equations (4.26),

(4.27) and (4.28) required for generating the nominal trajectory is given by

$$\dot{\bar{x}}_4 = 0 \quad (4.66)$$

Therefore, the state vector $\bar{x}(i)$ became 4-dimensional and is given by

$$\bar{x}(i) = \text{col} [\bar{x}_1(i), \bar{x}_2(i), \bar{x}_3(i), \bar{x}_4(i)] \quad (4.67)$$

The performance index to be minimized became

$$I = \sum_{i=0}^N Q [y(i) - \bar{x}_1(i) - \bar{x}_4(i)]^2 \quad (4.68)$$

Consequently, the equations (4.34), (4.35), (4.36) for (i) 's were replaced by the following equations.

$$\begin{aligned} \lambda_1(i-1) &= f_{\bar{x}(i)}^{11} \lambda_1(i) + f_{\bar{x}(i)}^{21} \lambda_2(i) + f_{\bar{x}(i)}^{31} \lambda_3(i) + f_{\bar{x}(i)}^{41} \lambda_4(i) \\ &\quad + 2 Q [y(i) - \bar{x}_1(i) - \bar{x}_4(i)] \end{aligned} \quad (4.69)$$

$$\lambda_2(i-1) = f_{\bar{x}(i)}^{12} \lambda_1(i) + f_{\bar{x}(i)}^{22} \lambda_2(i) + f_{\bar{x}(i)}^{32} \lambda_3(i) + f_{\bar{x}(i)}^{42} \lambda_4(i) \quad (4.70)$$

$$\lambda_3(i-1) = f_{\bar{x}(i)}^{13} \lambda_1(i) + f_{\bar{x}(i)}^{23} \lambda_2(i) + f_{\bar{x}(i)}^{33} \lambda_3(i) + f_{\bar{x}(i)}^{43} \lambda_4(i) \quad (4.71)$$

$$\begin{aligned} \lambda_4(i-1) &= f_{\bar{x}(i)}^{14} \lambda_1(i) + f_{\bar{x}(i)}^{24} \lambda_2(i) + f_{\bar{x}(i)}^{34} \lambda_3(i) + f_{\bar{x}(i)}^{44} \lambda_4(i) \\ &\quad + 2 Q [y(i) - \bar{x}_1(i) - \bar{x}_4(i)] \end{aligned} \quad (4.72)$$

The nominal trajectory $\bar{x}_1(i)$ and the Jacobian $f_{\bar{x}(i)}$ were

computed by numerical integration from the relevant equations.

The input-output data used here was the same as that for method

(a). Only the formulation of the problem was changed. The same

computational algorithm was followed for estimation and the

estimates of $x_1(0)$, $x_2(0)$, $x_3(0)$ and $x_4(0)$ are shown in Figures 4.7, 4.8 and 4.9 and Table 4.2. The results obtained by this method are also better than those of case I.

Method (c)

This method also involves the fourth state variable to represent the mean of noise but the plant equations are written in a different manner to improve convergence during estimation procedure.

Let a new variable $x_1'(i)$ be defined as

$$x_1'(i) = x_1(i) + x_4(i) \quad (4.73)$$

where $x_1(i)$ is the true state and $x_4(i)$ is the mean of noise as discussed earlier. It was seen in case I for noise having nonzero mean that the best fit of $\bar{x}_1(i)$ on $y(i)$ is away from the true trajectory $x_1(i)$ by the amount equal to the mean $x_4(i)$ of noise. In other words, the estimate of $x_1(i)$ was found to be $x_1'(i)$ giving an incorrect estimate. It was intuitively felt that if one attempted to obtain the estimate of trajectory $x_1'(i)$, better results could be obtained. Equation (4.73) is written in continuous-time as

$$\dot{x}_1' = \dot{x}_1 + \dot{x}_4 \quad (4.74)$$

Substituting for $x_1(i)$ from equation (4.73) in equation (4.18), one obtains

$$\dot{x}_1' = -x_1' x_2 + x_4 x_2 + x_2 x_3 \quad (4.75)$$

This equation, augmented by the equations (4.19), (4.20) and (4.62) complete the set of equations to describe the plant dynamics. Use of equation (4.73) in equation (4.65) gives

$$y(i) = x_1'(i) + n'(i) \quad (4.76)$$

In this context, the performance index is written as

$$I = \sum_{i=0}^N \Omega [y(i) - \bar{x}_1'(i)]^2 \quad (4.77)$$

where $\bar{x}_1'(i)$ is the nominal trajectory obtained by numerical integration of the equation

$$\dot{\bar{x}}_1' = -\bar{x}_1' \bar{x}_2 + \bar{x}_4 \bar{x}_2 + \bar{x}_2 \bar{x}_3 u \quad (4.78)$$

supplemented by equations (4.27), (4.28) and (4.66). The equations (4.34), (4.35) and (4.36) for $\lambda(i)$'s were replaced by the following equations.

$$\begin{aligned} \lambda_1(i-1) = & f_{\bar{x}(i)}^{11} \lambda_1(i) + f_{\bar{x}(i)}^{21} \lambda_2(i) + f_{\bar{x}(i)}^{31} \lambda_3(i) + f_{\bar{x}(i)}^{41} \lambda_4(i) \\ & + 2 \Omega [y(i) - \bar{x}_1'(i)] \end{aligned} \quad (4.79)$$

$$\lambda_2(i-1) = f_{\bar{x}(i)}^{12} \lambda_1(i) + f_{\bar{x}(i)}^{22} \lambda_2(i) + f_{\bar{x}(i)}^{32} \lambda_3(i) + f_{\bar{x}(i)}^{42} \lambda_4(i) \quad (4.80)$$

$$\lambda_3(i-1) = f_{\bar{x}(i)}^{13} \lambda_1(i) + f_{\bar{x}(i)}^{23} \lambda_2(i) + f_{\bar{x}(i)}^{33} \lambda_3(i) + f_{\bar{x}(i)}^{43} \lambda_4(i) \quad (4.81)$$

$$\lambda_4(i-1) = f_{\bar{x}(i)}^{14} \lambda_1(i) + f_{\bar{x}(i)}^{24} \lambda_2(i) + f_{\bar{x}(i)}^{34} \lambda_3(i) + f_{\bar{x}(i)}^{44} \lambda_4(i) \quad (4.82)$$

The elements of Jacobian matrix $f_{\bar{x}(i)}$ were obtained using equation (3.46) wherein the matrix $g_{\bar{x}}$ is obtained from equations (4.78), (4.27), (4.28) and (4.66). The same computational algorithm was used again. As expected, the results obtained by this method are slightly better than those obtained by methods (a) and (b) of case II as is evident from Figures 4.7, 4.8 and

4.9 and Table 4.2.

Table 4.2 Estimated Values of Initial States for a Computer-Simulated System Similar to the Open-loop Plant -
CASE II.

	$x_1(0)$	$x_2(0)$	$x_3(0)$	$x_4(0)$ or $\frac{n}{m}$
(1) True Values	0.2	0.4	2.0	- 0.058
Estimated Values				
(2) Method (a)	0.196	0.427	1.914	- 0.046
(3) Method (b)	0.187	0.426	1.916	- 0.045
(4) Method (c), $x_1'(0) =$	0.155	0.416	1.922	- 0.046
	$\therefore x_1(0) = x_1'(0) - x_4(0)$ $= 0.155 + 0.046$ $= 0.202$			

It can be seen that method of case II(c) gave results slightly better than those in case II(a). But case II(c) involved more computational time in computing the Jacobian $f_{\frac{n}{m}} \text{ on } \bar{x}(i)$ account of the additional state variable $x_4(i)$. In view of this, method II(a) was preferred for the estimation of parameters from the actual operating input-output data as is discussed in the following section. The time required on IBM 7094 for each of these programs was about 2 to 3 minutes.

It was also observed that the computational algorithm developed here worked equally well for estimation of any first order plant (i.e. plant having ANY gain and time constant other than those assumed here).

4.5 Estimation from Actual Operating Data of the Open-loop Plant

Having ensured the feasibility of our estimation method with a suitable computational algorithm with input-output data of a computer-simulator system, the method was then applied to the turbo-alternator data. The actual data was obtained for 10 minutes giving 4800 samples of input $\Delta p'$ (i.e. power load fluctuations) at the rate of 8 samples/second and 1200 samples of output $\Delta \omega'$ (i.e. frequency fluctuations) with a sampling period of 0.5 seconds. Since the open-loop plant acts like a low pass filter (on account of large moment of inertia of the turbo-alternator rotor), high frequency fluctuations in $\Delta p'$ do not reflect in the output $\Delta \omega'$. The sampling interval for $\Delta \omega'$ was therefore chosen longer than that for $\Delta p'$. This also reduces measurement labour and cost. The average operating levels were removed from both input and output data because the variations otherwise were very small as compared to the operating levels. This was necessary to obtain better correspondence between variations in input and output.

Early experiments using AMRK or other simpler subroutines for integration over the entire 10 minutes span of data per every iteration showed that it took a long time even for few iterations. A need for faster subroutine for integration was felt. The differential equations (4.26), (4.27) and (4.28) were transformed into difference equations considering linear interpolation between successive samples for input. The difference equations thus obtained for the nonnominal trajectory are

$$\begin{aligned} \bar{x}_1(i+1) = & e^{-\bar{x}_2(i)T} \bar{x}_1(i) + \bar{x}_3(i) u(i+1) \left[1 - \frac{1}{\bar{x}_2(i)T} + \frac{e^{-\bar{x}_2(i)T}}{\bar{x}_2(i)T} \right] \\ & + \bar{x}_3(i) u(i) \left[\frac{1}{\bar{x}_2(i)T} - e^{-\bar{x}_2(i)T} - \frac{e^{-\bar{x}_2(i)T}}{\bar{x}_2(i)T} \right] \\ & i = 0, 1, \dots, N \end{aligned} \quad (4.83)$$

$$\bar{x}_2(i+1) = \bar{x}_2(i) \quad i = 0, 1, \dots, N \quad (4.84)$$

$$\bar{x}_3(i+1) = \bar{x}_3(i) \quad i = 0, 1, \dots, N \quad (4.85)$$

where 'T' is the sampling period. Equations (4.83) to (4.85) were used in generating the nominal trajectory $\bar{x}_1(i)$ starting with the initial guess on $\bar{x}_1(0)$, $\bar{x}_2(0)$ and $\bar{x}_3(0)$. It is easy to obtain Jacobian $f_{\bar{x}(i)}$ from these difference equations.

Thus by virtue of equation (3.15), one obtains

$$f_{\bar{x}(i)}^{11} = e^{-\bar{x}_2(i)T} \quad (4.86)$$

$$\begin{aligned} f_{\bar{x}(i)}^{12} = & -T e^{-\bar{x}_2(i)T} \bar{x}_1(i) + \bar{x}_3(i) [u(i+1) - u(i)] \left[\frac{1}{\bar{x}_2(i)T} \right. \\ & \left. - \frac{e^{-\bar{x}_2(i)T}}{\bar{x}_2(i)T} - \frac{e^{-\bar{x}_2(i)T}}{\bar{x}_2(i)} \right] + \bar{x}_3(i) u(i) T e^{-\bar{x}_2(i)T} \end{aligned} \quad (4.87)$$

$$f_{\bar{x}(i)}^{13} = u(i+1) - \frac{[u(i+1) - u(i)] [1 - e^{-\bar{x}_2(i)T}]}{\bar{x}_2(i)T} - e^{-\bar{x}_2(i)T} u(i) \quad (4.88)$$

$$f_{\bar{x}(i)}^{21} = f_{\bar{x}(i)}^{23} = f_{\bar{x}(i)}^{31} = f_{\bar{x}(i)}^{32} = 0 \quad (4.89)$$

$$f_{\bar{x}(i)}^{22} = f_{\bar{x}(i)}^{33} = 1 \quad (4.90)$$

Equations (4.86) to (4.90) were used in computing the Jacobian matrix required for estimation procedure. Since the rate of sampling of input data was 4 times that of the output data, the

subroutine using the above equations with $T = 0.125$ secs. was required to be CALLED four times to reach the next sample of nominal trajectory $\bar{x}_1(i)$ to compare the observed output $y(i)$ at the corresponding sampling instant. This increased the computation time 4 times. The computation time could be reduced by either of the following two types of high frequency filtering.

(1) High frequency filtering by modifying the input data $\Delta p'$ (i.e. $u(i)$) by taking average over four samples, i.e.

$$\text{filtered } u(i) = \frac{1}{4} \sum_{k=1}^4 u(i+k-1) \quad ; \quad i = 0, 4, 8, \dots, N \quad (4.91)$$

This gave the modified input data with a sampling interval of 0.5 sec. and reduced the number of samples to 1200, the same as that for the observed output $\Delta \omega'$, i.e. $y(i)$. This amounted to high frequency (h.f.) filtering²¹ of the input data with a cut-off frequency of 2.0 c/s as shown below.

$$\text{Filter function } F(f) = \frac{1}{k+1} \left[\frac{\sin\left\{\frac{(k+1)\omega \Delta t}{2}\right\}}{\sin\left\{\frac{\omega \Delta t}{2}\right\}} \right] \quad (4.92)$$

where

f = frequency in c/s

$k+1$ = Number of data points averaged (4 in the present case)

Δt = Sampling period (0.125 in the present case)

$F(f)$ = gain of the filter at frequency f , which is maximum at $f=0$ and becomes zero at $f=f_c$, the cut-off frequency.

The cut-off frequency for the filter can be easily computed as 2.0 c/s by equating to zero, the numerator of the right hand side of equation (4.92).

(2) High frequency filtering by modifying the input data $u(i)$ by taking average over eight samples and modifying the output data $y(i)$ by taking average over two samples, i.e.

$$\text{filtered } u(i) = \frac{1}{8} \sum_{k=1}^8 u(i+k-1) \quad ; \quad i = 0, 8, 16, \dots \quad (4.93)$$

and

$$\text{filtered } y(i) = \frac{1}{2} \sum_{k=1}^2 y(j+k-1) \quad ; \quad j = 0, 2, 4, \dots \quad (4.94)$$

This gave the filtered input and output data with a sampling interval of 1.0 second and reduced the number of samples to 600 for both. Substituting for $k+1 = 8$ and $\Delta t = 0.125$ sec. for input data and $k+1 = 2$ and $\Delta t = 0.5$ for the output data in equation (4.92), the cut-off frequency can be obtained as 1.0 c/s for both.

The open-loop plant has a time-constant⁹⁰ of about 2.5 secs. which gives the corner frequency $\omega_c = 0.5$ rad/sec or $f_c = 0.08$ c/s. Therefore, no appreciable information was lost by using h.f. filtered data having f_c equal to either 2.0 or 1.0 c/s. Indeed, some experiments did show that the estimator without or with h.f. filtering ($f_c = 2.0$ c/s), using the same length of time of data, gave the same results. The results obtained using h.f. filter with $f_c = 1.0$ c/s gave results little different but the computer time taken was the least because the number of measurements were reduced to 600. However, considering better accuracy, the h.f. filtering with $f_c = 2.0$ c/s and 1200 filtered data points was considered suitable.

The method used for estimation with actual data was the same as Method (a) of case II in section 4.4 with the only difference that the simulated data was replaced by the actual one. The

initial guesses for the initial conditions were $\bar{x}_1(0) = y(0)$; $\bar{x}_2(0) = 0.1$; $\bar{x}_3(0) = -0.1$. Since the increase in power load would result in decrease in frequency, the gain of open-loop plant transfer function was expected to have negative value. The initial guess for $\bar{x}_3(0)$ was taken as -0.1 so that it would converge in the right direction in the very early stages instead of taking a different course in the beginning and then turning back in the right direction, thus saving computation time. The following five experiments were made for estimating the gain and the time-constant for the open-loop plant from normal operating data.

(1) Estimation using High Frequency Filtered Data ($f_c = 2.0$ c/s) with Means Deducted.

The means for both input and output were computed and subtracted from their respective data. This removed the average operating levels leaving only the variations. The convergence of $\bar{x}_1(0)$, $\bar{x}_2(0)$ and $\bar{x}_3(0)$ starting from initial guesses are shown by curves marked "(1)" in Figures 4.10, 4.11 and 4.12 respectively. The estimated values are also shown in Table 4.3. The estimated values $x_2(0) = 0.445$ and $x_3(0) = -0.465$ were found to be different (particularly $x_3(0)$) from their expected values $x_2(0) = 1/\gamma_m = 0.4$, $x_3(0) = 1/D' = 2.19$ c/s / p.u. obtained earlier by power spectral analysis.⁹⁰ An unaccounted l.f. source was suspected to be present in the form of dynamic noise which could not be measured at the input. However, its effect appeared in the output measurements and this gave different estimated values. The estimation method developed in chapter III is equipped to take care of only the additive noise at the output and not the dynamic noise generated within the system. The dynamic noise is usually correlated and can not be tackled as easily as the additive noise at the output, in the general formulation of estimation scheme of chapter III. Had the dynamic noise been in the h.f. range, it would have disappeared with h.f. filtering. Thus digital l.f. filtering of both input and output data was necessary to remove this l.f. dynamic noise. The following four

experiments were performed to show the effect of different l.f. filters.

(2) Using First Differences for Wide Band Low Frequency Filtering.

A very wide band l.f. filtering²¹ was first tried on the h.f. filtered ($f_c = 2.0$ c/s) data using the first differences, i.e.

$$\text{filtered } u(i) = u(i+1) - u(i) \quad (4.95)$$

and

$$\text{filtered } y(i) = y(i+1) - y(i) \quad (4.96)$$

This gave the estimate of $x_2(0)$ and $x_3(0)$ to be 0.209 and -2.130 respectively (depicted in Figures 4.10, 4.11 and 4.12 and Table 4.3).

(3) Using Low Frequency Filtering²¹ with $f_c = 0.025$ c/s.

This was obtained by applying the following treatment to the h.f. filtered data

$$\text{filtered } u(i) = u(i) - \frac{1}{80} \sum_{k=1}^{80} u(i+k-1) \quad (4.97)$$

and

$$\text{filtered } y(i) = y(i) - \frac{1}{80} \sum_{k=1}^{80} y(i+k-1) \quad (4.98)$$

The corresponding filter gain function is

$$F(f) = 1.0 - \frac{1}{k+1} \left[\frac{\sin\left\{\frac{(k+1)\omega\Delta t}{2}\right\}}{\sin\left\{\frac{\omega\Delta t}{2}\right\}} \right] \quad (4.99)$$

Here $k+1 = 80$ and $\Delta t = 0.5$ sec. The l.f. filter response is plotted in Fig. 4.13. The estimated values as can be seen from Figures 4.10, 4.11 and 4.12 and Table 4.3 are $x_2(0) = 0.345$ and $x_3(0) = -1.254$.

(4) Using Low Frequency Filtering with $f_c = 0.05$ c/s.

This was accomplished by using the formulas

$$\text{filtered } u(i) = u(i) - \frac{1}{40} \sum_{k=1}^{40} u(i+k-1) \quad (4.100)$$

and

$$\text{filtered } y(i) = y(i) - \frac{1}{40} \sum_{k=1}^{40} y(i+k-1) \quad (4.101)$$

The cut-off frequency f_c can be easily found from equation (4.99) by substituting $k+1 = 40$ and $\Delta t = 0.5$ sec. The filter response is shown in Fig. 4.13. As a result of this filtering, the estimated values were changed to $x_2(0) = 0.250$ and $x_3(0) = -2.158$. (Figures 4.10, 4.11, 4.12 and Table 4.3).

(5) Using Low Frequency Filtering with $f_c = 0.1$ c/s.

This was done by modifying the h.f. filtered data in the following way.

$$\text{filtered } u(i) = u(i) - \frac{1}{20} \sum_{k=1}^{20} u(i+k-1) \quad (4.102)$$

and

$$\text{filtered } y(i) = y(i) - \frac{1}{20} \sum_{k=1}^{20} y(i+k-1) \quad (4.103)$$

The filter gain is plotted in Fig. 4.13 by taking $k+1 = 20$ and $\Delta t = 0.5$ sec. in equation (4.99). The estimated values are depicted in Figures 4.10, 4.11 and 4.12 and Table 4.3 are $x_2(0) = 0.234$ and $x_3(0) = -2.617$.

Table 4.3 Comparative Statement of Estimated Values of $x_2(0)$ and $x_3(0)$ Obtained by Different Low Frequency Filterings.

Type of Filtering	Estimated	
	$x_2(0)$	$x_3(0)$
(1) With means deducted	0.445	-0.465
(2) Using first differences	0.209	-2.130
(3) Using l.f. filtering, $f_c = 0.025$ c/s	0.345	-1.254
(4) Using l.f. filtering, $f_c = 0.05$ c/s	0.250	-2.158
(5) Using l.f. filtering, $f_c = 0.1$ c/s	0.234	-2.517

It was concluded that l.f. filtering with $f_c = 0.05$ c/s was considered to be the best suitable filter and it gave estimated values closest to those expected. The estimated values of $x_2(0)$ and $x_3(0)$ are 0.25 and -2.158 respectively. Referring to equations (4.16) and (4.17), the values of τ_m and D' are given by

$$\tau_m = 1/x_2(0) = 1/0.25 = 4.0 \text{ secs.} \quad (4.104)$$

$$D' = 1/x_3(0) = 1/(-2.158) = -0.463 \quad (4.105)$$

Using equation (4.10), one gets

$$\begin{aligned} D &= \frac{1200}{10^4} D' \\ &= -1200 \times 0.463/10^4 \\ &= -0.0556 \text{ p.u. / c/s} \end{aligned} \quad (4.106)$$

The estimation procedure developed for simulated conditions and later used for estimation from actual operating data showed no difficulty in convergence. The fact that the estimated values of parameters corresponded to the only minimum of I was verified by computing I for different values of $\bar{x}_2(0)$ and $\bar{x}_3(0)$. The l.f. dynamic noise gave some trouble but this difficulty was

overcome by using suitable filtering. Having obtained experience and confidence in the method of estimation for the first order open-loop plant, the technique was applied to a second order closed-loop plant (with the feedback loop employing governor closed - Fig. 4.1) as will be discussed in Chapter V.

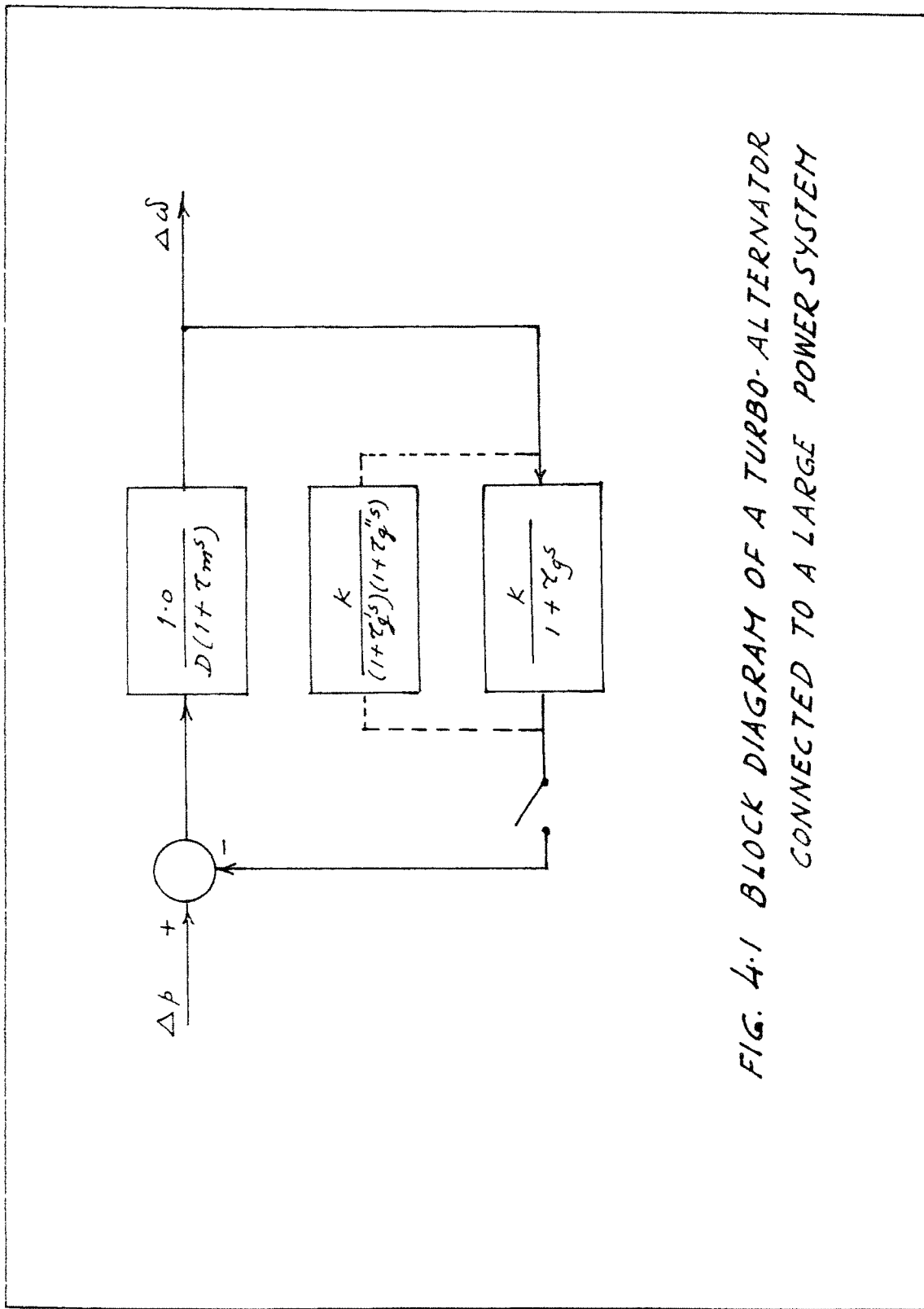


FIG. 4.1 BLOCK DIAGRAM OF A TURBO-ALTERNATOR
CONNECTED TO A LARGE POWER SYSTEM

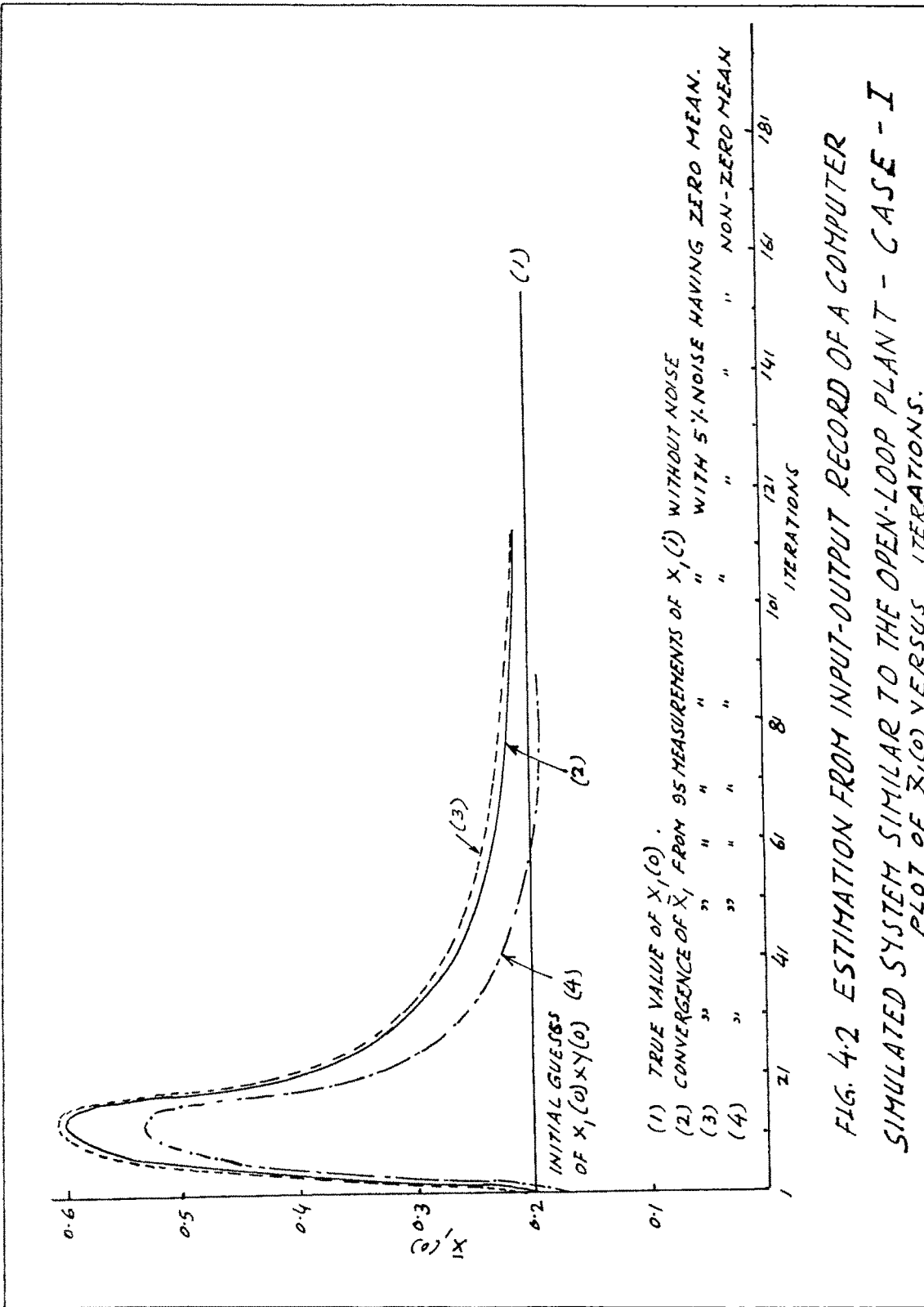


FIG. 4.2 ESTIMATION FROM INPUT-OUTPUT RECORD OF A COMPUTER SIMULATED SYSTEM SIMILAR TO THE OPEN-LOOP PLANT - CASE - I
 PLOT OF $\bar{X}_1(0)$ VERSUS ITERATIONS.

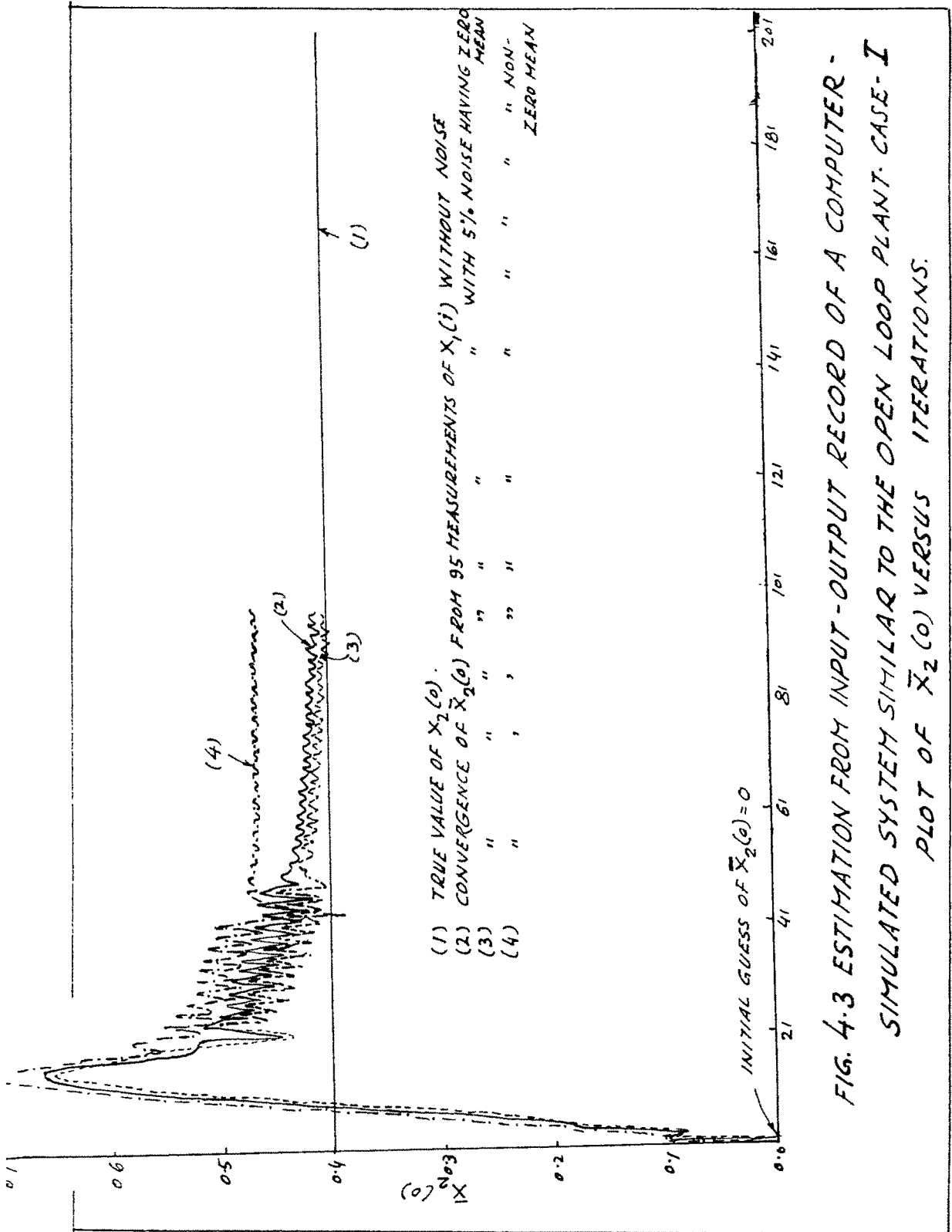


FIG. 4.3 ESTIMATION FROM INPUT-OUTPUT RECORD OF A COMPUTER -
 SIMULATED SYSTEM SIMILAR TO THE OPEN LOOP PLANT. CASE - I
 PLOT OF $\bar{X}_2(0)$ VERSUS ITERATIONS.

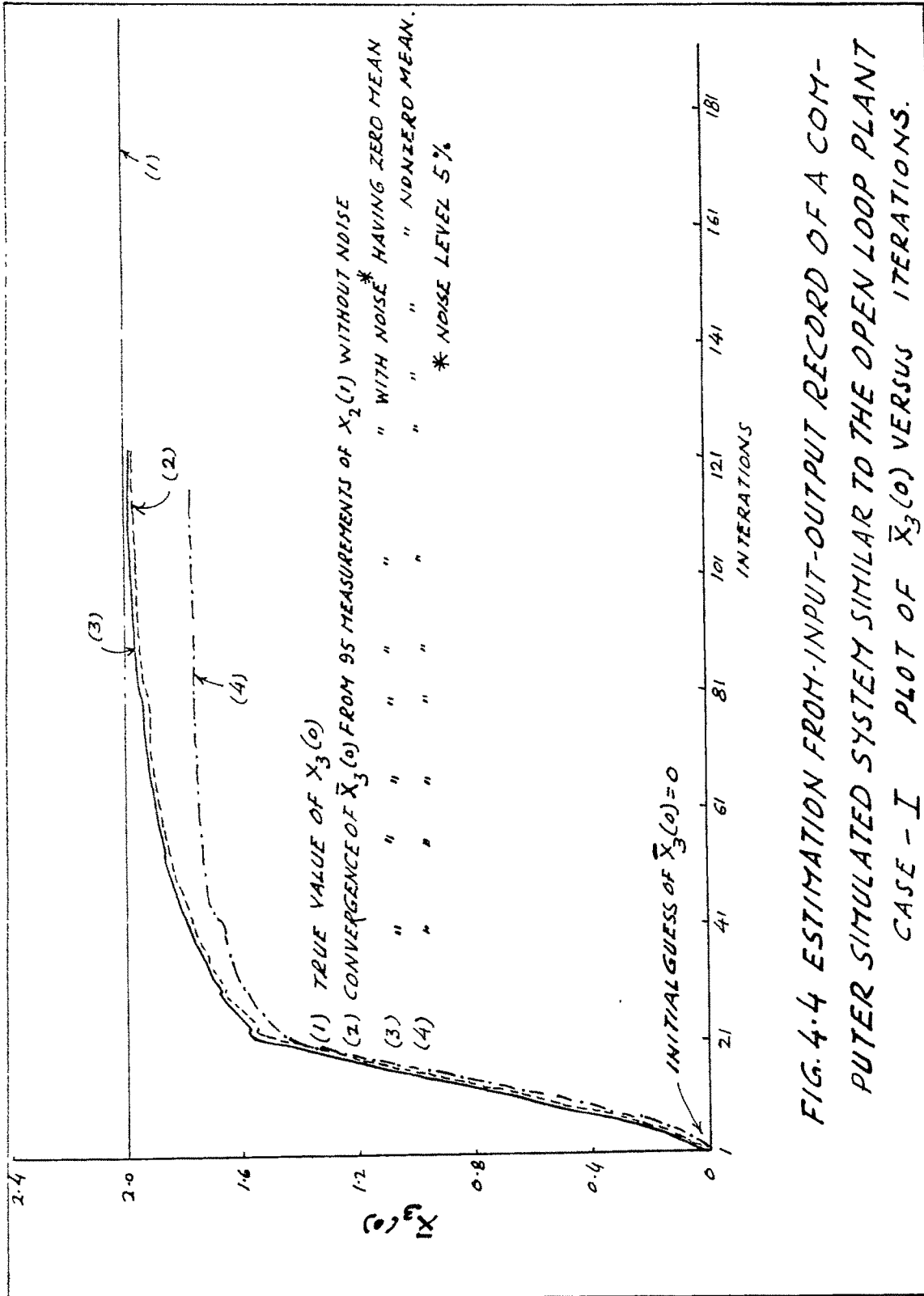


FIG. 4.4 ESTIMATION FROM INPUT-OUTPUT RECORD OF A COMPUTER SIMULATED SYSTEM SIMILAR TO THE OPEN LOOP PLANT
 CASE - I PLOT OF $\bar{X}_3(0)$ VERSUS ITERATIONS.

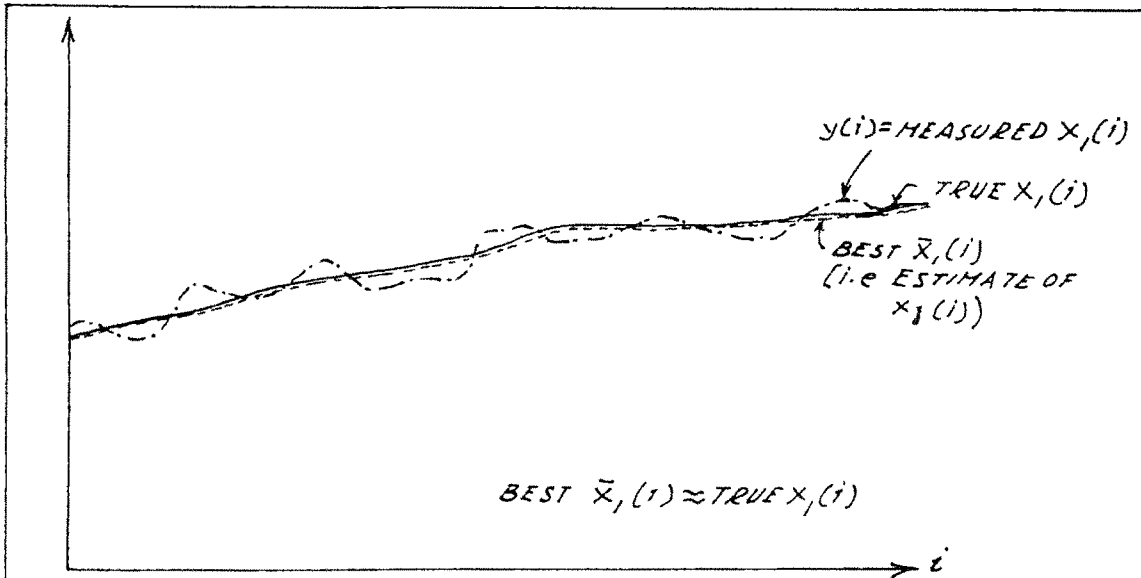


FIG. 4.5 LEAST SQUARES ESTIMATE FROM MEASUREMENTS WITH NOISE HAVING ZERO MEAN.

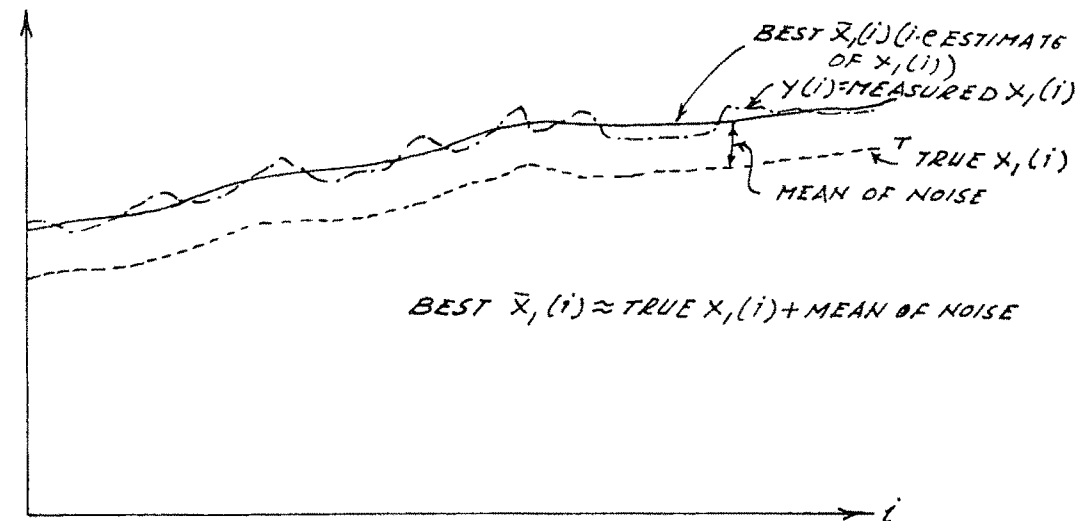


FIG. 4.6 LEAST SQUARES ESTIMATE FROM MEASUREMENTS WITH NOISE HAVING NON ZERO MEAN.

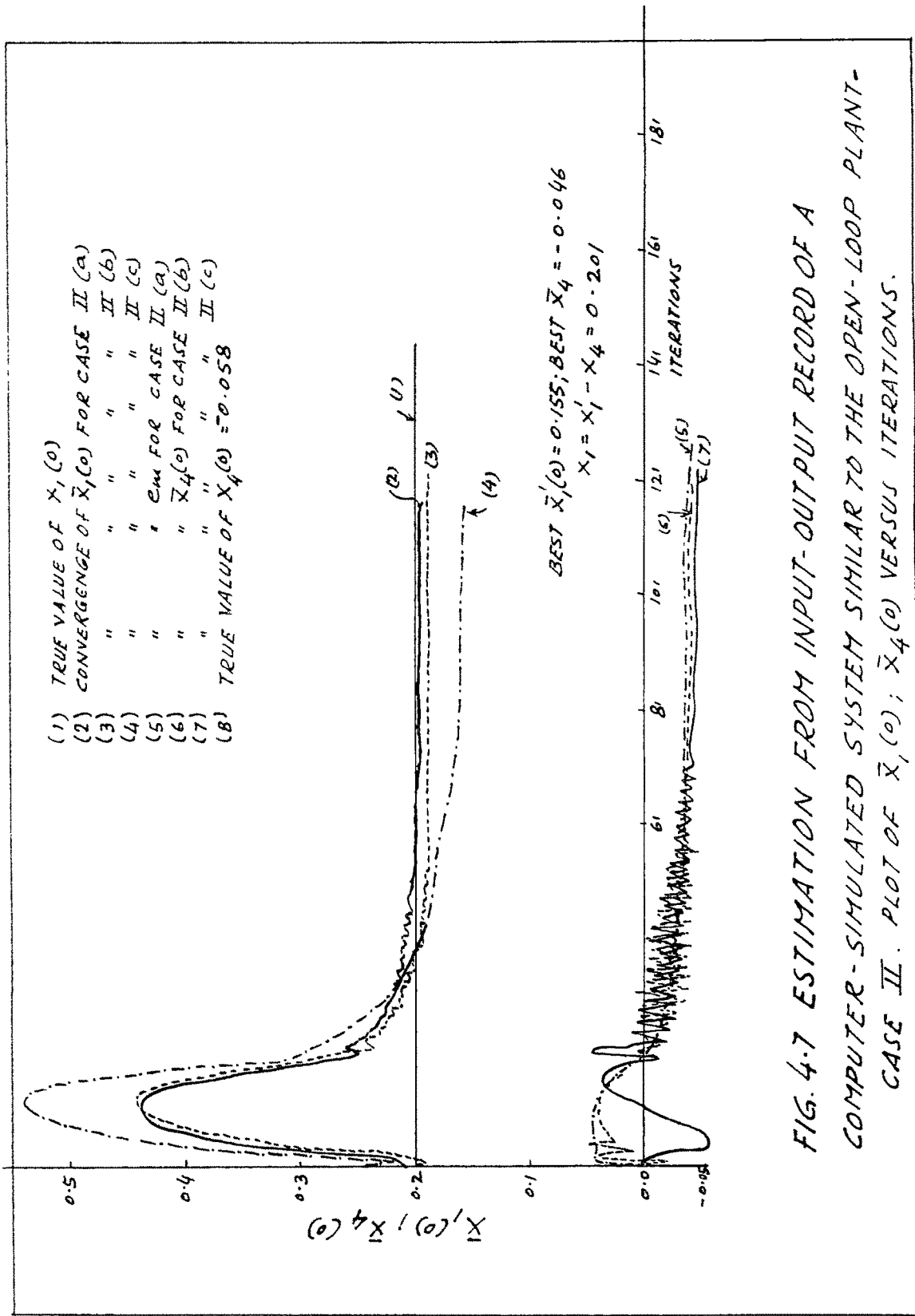
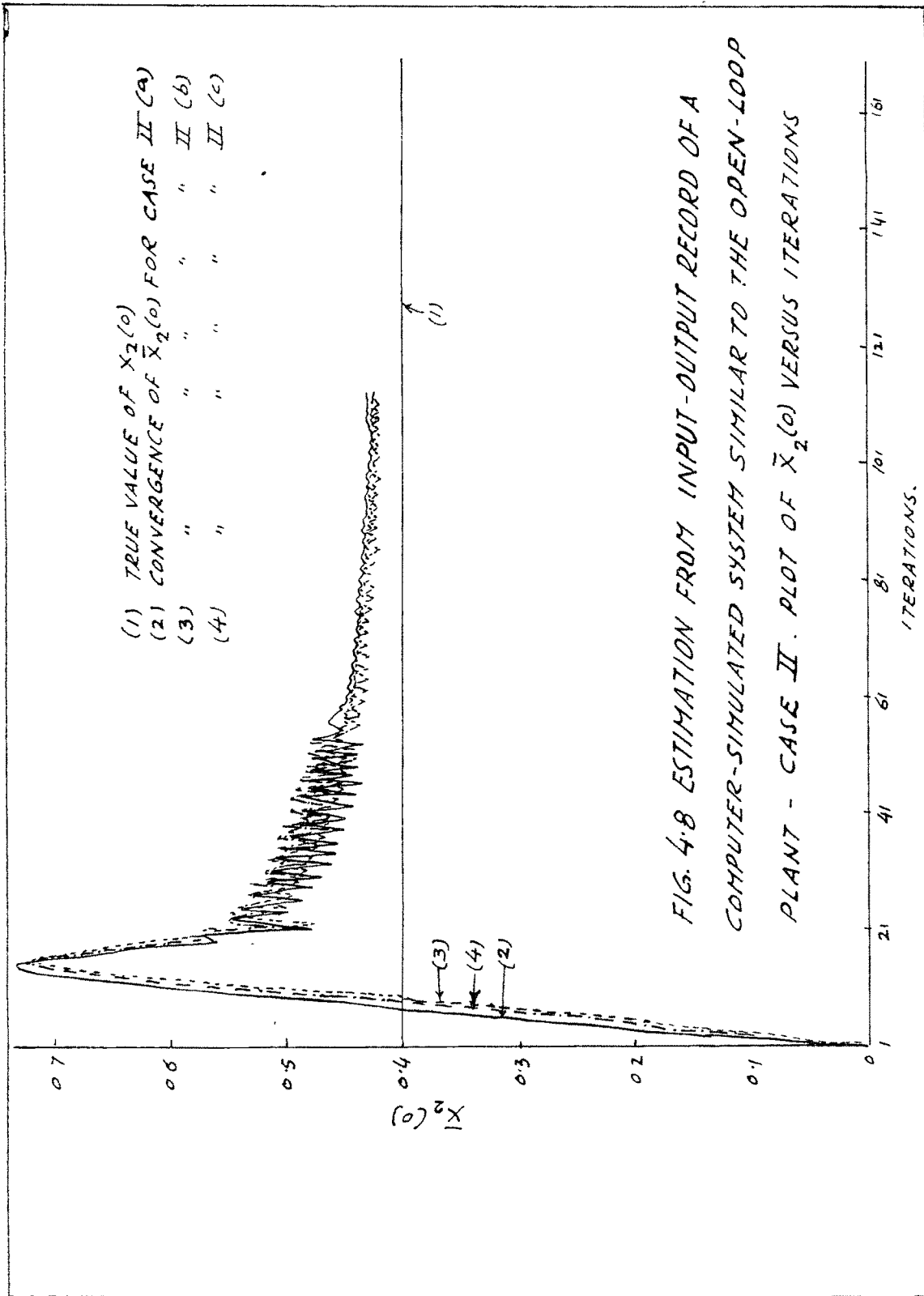


FIG. 4-7 ESTIMATION FROM INPUT-OUTPUT RECORD OF A COMPUTER-SIMULATED SYSTEM SIMILAR TO THE OPEN-LOOP PLANT-CASE II. PLOT OF $\bar{X}_1(0)$; $\bar{X}_4(0)$ VERSUS ITERATIONS.



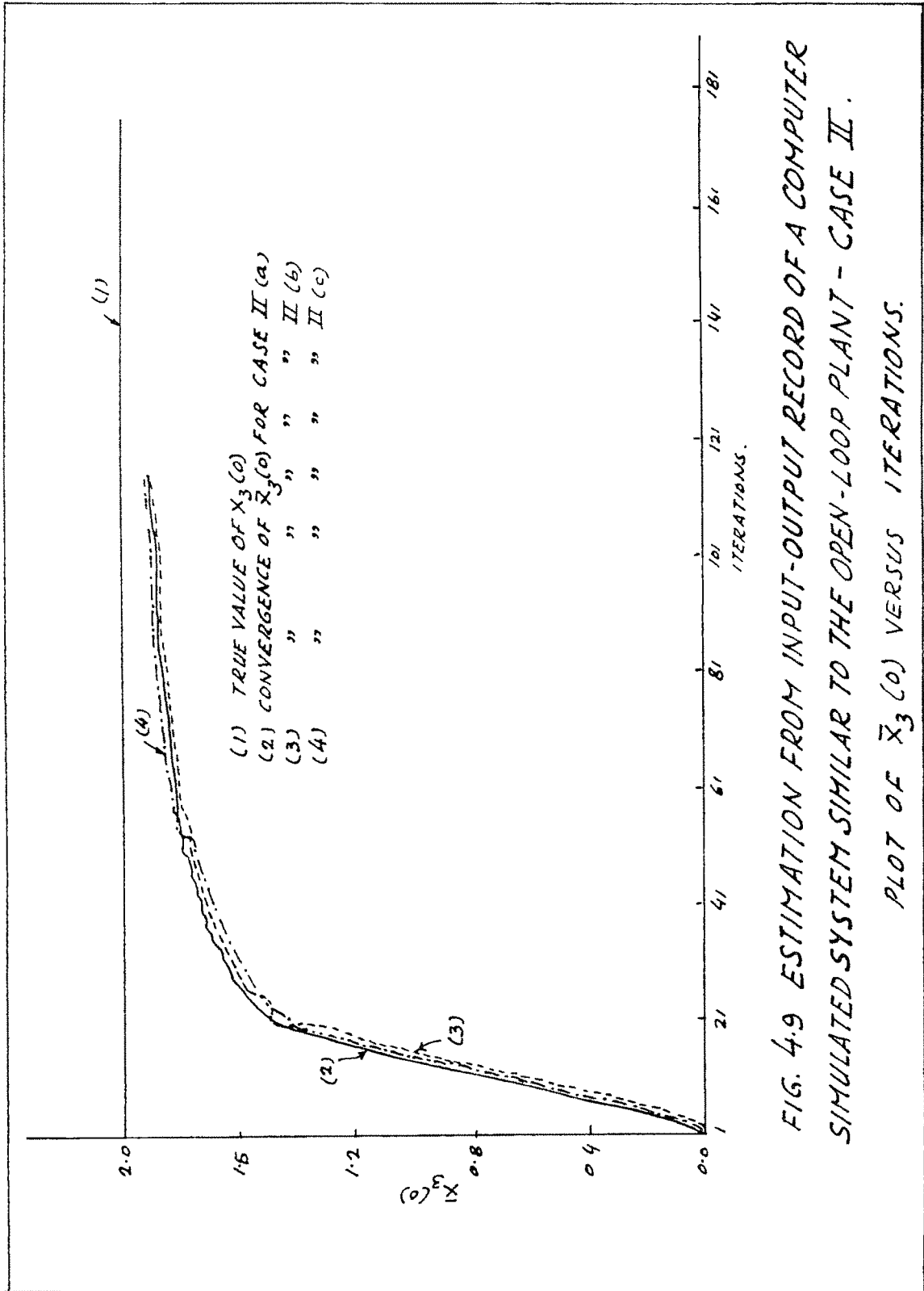


FIG. 4.9 ESTIMATION FROM INPUT-OUTPUT RECORD OF A COMPUTER SIMULATED SYSTEM SIMILAR TO THE OPEN-LOOP PLANT - CASE II.

PLOT OF $\bar{X}_3(0)$ VERSUS ITERATIONS.

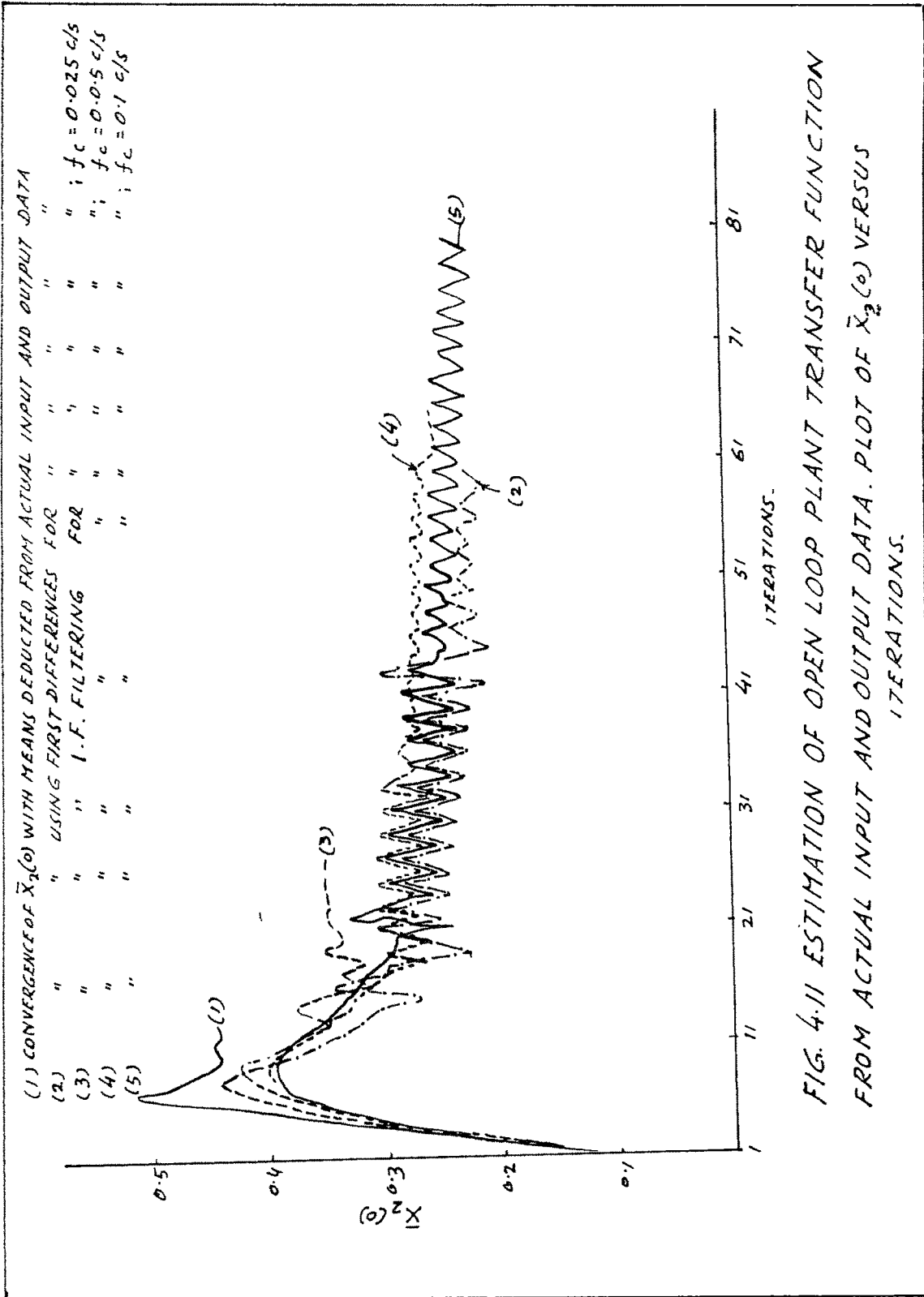


FIG. 4.11 ESTIMATION OF OPEN LOOP PLANT TRANSFER FUNCTION FROM ACTUAL INPUT AND OUTPUT DATA. PLOT OF $\bar{X}_2(s)$ VERSUS ITERATIONS.

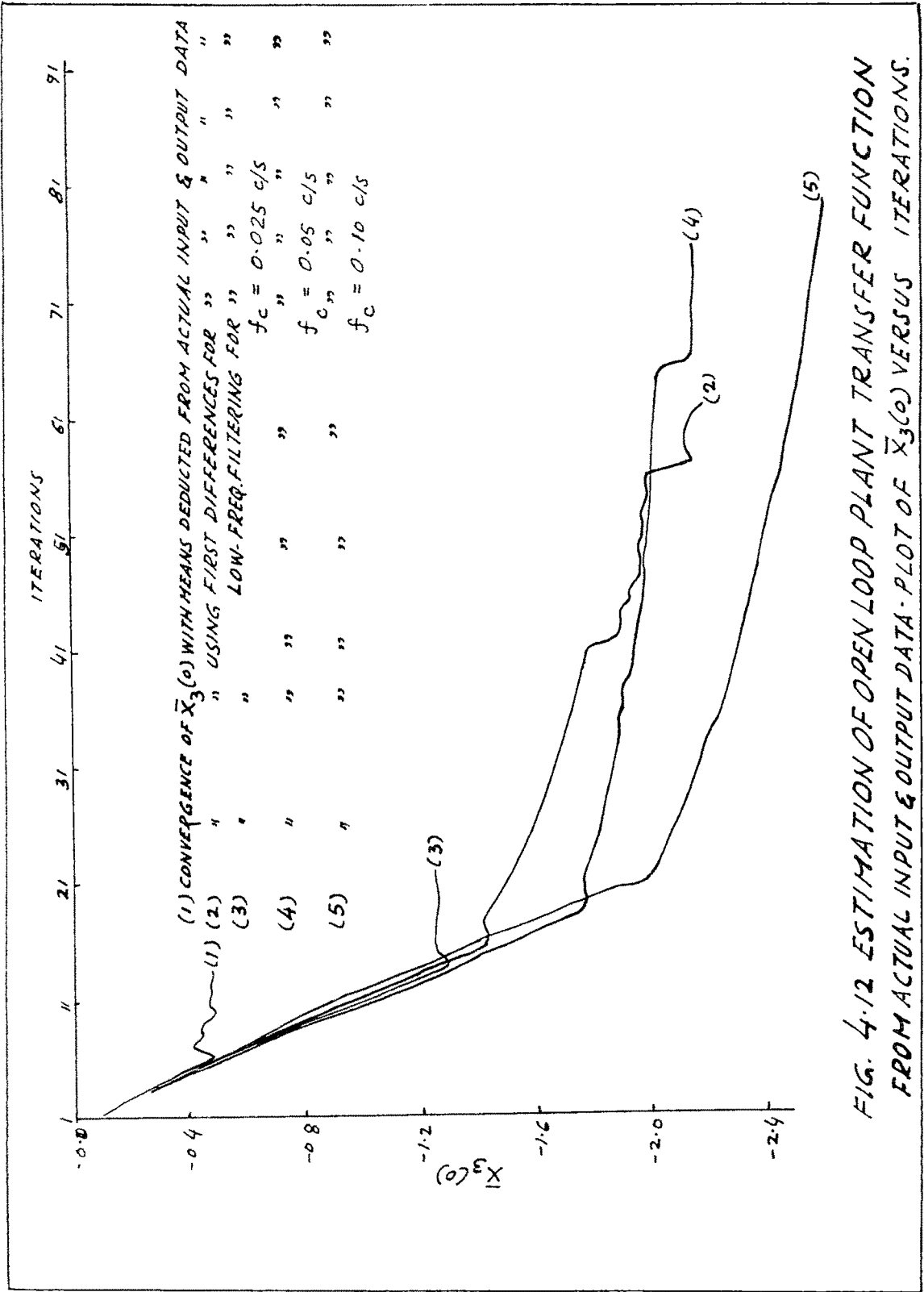


FIG. 4.12 ESTIMATION OF OPEN LOOP PLANT TRANSFER FUNCTION FROM ACTUAL INPUT & OUTPUT DATA. PLOT OF $\bar{X}_3(0)$ VERSUS ITERATIONS.

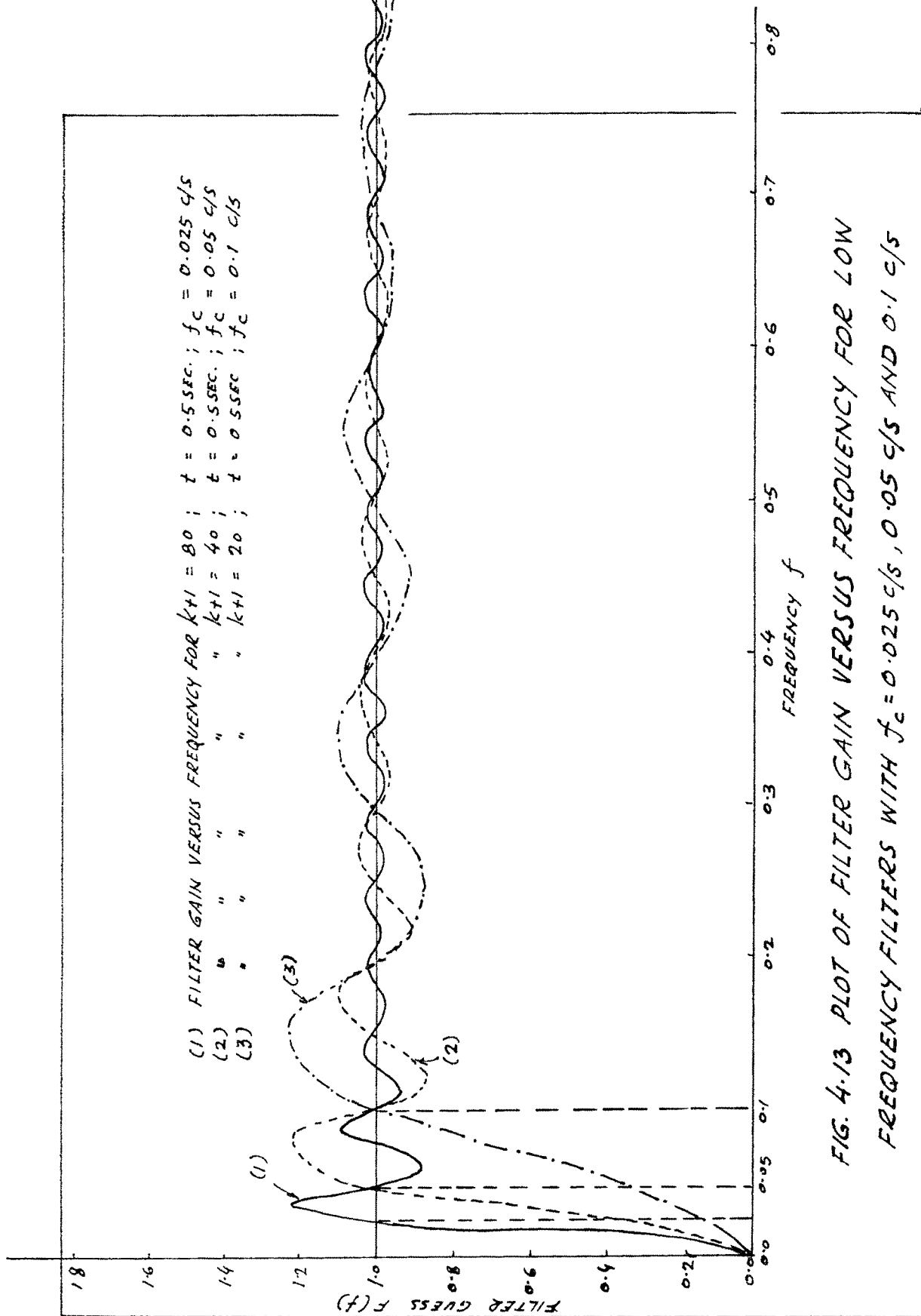


FIG. 4.13 PLOT OF FILTER GAIN VERSUS FREQUENCY FOR LOW FREQUENCY FILTERS WITH $f_c = 0.025 \text{ C/S}$, 0.05 C/S AND 0.1 C/S